


DHCR24 Insufficiency Promotes Vascular Endothelial Cell Senescence and Endothelial Dysfunction via Inhibition of Caveolin-1/ERK Signaling

Han Li, MM,¹ Zhen Yang, MD,^{1,2} Wukaiyang Liang, BM,¹ Hao Nie, MD,^{1,2} Yuqi Guan, MD,^{1,2} Ni Yang, MM,¹ Tianyi Ji, BM,¹ Yu Liu, MD,^{1,2} Yi Huang, MS,^{1,2} Le Zhang, PhD,^{1,2}  Jinhua Yan, MD,^{1,2,*} and Cuntai Zhang, MD^{1,2,*}

¹Key Laboratory of Vascular Aging, Ministry of Education, Tongji Hospital of Tongji Medical College, Huazhong University of Science and Technology, Wuhan, People's Republic of China.

²Department of Geriatrics, Tongji Hospital of Tongji Medical College, Huazhong University of Science and Technology, Wuhan, PR China.

*Address correspondence to: Jinhua Yan, MD. E-mail: yanjinhua2013@outlook.com; Cuntai Zhang, MD. E-mail: ctzhang@tjh.tjmu.edu.cn

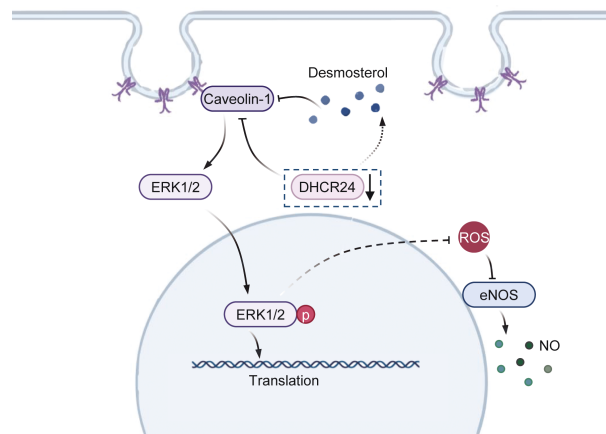
Decision Editor: Gustavo Duque, MD, PhD, FRACP, FGSA (Biological Sciences Section)

Abstract

Endothelial cells (ECs) senescence is critical for vascular dysfunction, which leads to age-related disease. DHCR24, a 3 β -hydroxysterol δ 24 reductase with multiple functions other than enzymatic activity, has been involved in age-related disease. However, little is known about the relationship between DHCR24 and vascular ECs senescence. We revealed that DHCR24 expression is chronologically decreased in senescent human umbilical vein endothelial cells (HUVECs) and the aortas of aged mice. ECs senescence in endothelium-specific DHCR24 knockout mice was characterized by increased P16 and senescence-associated secretory phenotype, decreased SIRT1 and cell proliferation, impaired endothelium-dependent relaxation, and elevated blood pressure. In vitro, DHCR24 knockdown in young HUVECs resulted in a similar senescence phenotype. DHCR24 deficiency impaired endothelial migration and tube formation and reduced nitric oxide (NO) levels. DHCR24 suppression also inhibited the caveolin-1/ERK signaling, probably responsible for increased reactive oxygen species production and decreased eNOS/NO. Conversely, DHCR24 overexpression enhanced this signaling pathway, blunted the senescence phenotype, and improved cellular function in senescent cells, effectively blocked by the ERK inhibitor U0126. Moreover, desmosterol accumulation induced by DHCR24 deficiency promoted HUVECs senescence and inhibited caveolin-1/ERK signaling. Our findings demonstrate that DHCR24 is essential in ECs senescence.

Keywords: Caveolin-1/ERK, Desmosterol, DHCR24, Vascular dysfunction, Vascular endothelial cell senescence

Graphical Abstract



Age-related cardio-vascular disease is the leading cause of death among older people in developed countries (1,2). Vascular aging significantly contributes to age-related vascu-

lar disorders (3,4). Endothelial cells (ECs), as a monolayer lining the inner layer of blood vessels, maintain physiological homeostasis and regulate organ function (5). Recent research

Received: September 25 2023; Editorial Decision Date: February 15 2024.

© The Author(s) 2024. Published by Oxford University Press on behalf of The Gerontological Society of America.

This is an Open Access article distributed under the terms of the Creative Commons Attribution-NonCommercial License (<https://creativecommons.org/licenses/by-nc/4.0/>), which permits non-commercial re-use, distribution, and reproduction in any medium, provided the original work is properly cited. For commercial re-use, please contact journals.permissions@oup.com

indicates that senescent ECs are associated with endothelial dysfunction, which increases the risk of age-related vascular diseases (5–7). However, the underlying mechanisms of ECs senescence and endothelial dysfunction remain unknown.

Endothelial cells senescence is a pathophysiological process characterized by structural and functional changes (8,9). Senescent ECs exhibit typical features, such as decreased nitric oxide (NO) bioavailability, cell cycle arrest, decreased proliferation, increased senescence-associated- β -galactosidase (SA- β -gal) activity, senescence-associated secretory phenotype (SASP), and expression of senescence-associated proteins (P16 and SIRT1) (6,10,11). ECs senescence and endothelial dysfunction are primarily caused by oxidative stress and inflammation (5). Nonetheless, the precise molecular regulatory mechanisms remain unknown.

DHCR24 is a xanthine adenine dinucleotide-dependent oxidoreductase, β -hydroxysterol δ 24 reductase, and the final reactive enzyme catalyzing cholesterol synthesis from desmosterol (12,13). DHCR24 is selectively down-regulated in brain regions affected by Alzheimer's disease (AD), the most common age-related neurodegenerative disease (14). Similarly, cholesterol synthesis is reduced in the aged human brain and aged mouse brain (15). Down-regulated DHCR24 is probably associated with aging, but evidence linking cause and effect is lacking. Recent studies indicated that DHCR24 has more complex effects than enzymatic activity, such as modulating oxidative stress (12). Down-regulated DHCR24 may contribute to endothelial cellular senescence because oxidative stress is a known cellular senescence mechanism.

Caveolin-1, a hallmark structural protein of caveolae, is found abundantly in ECs and specialized plasma membrane subdomains. It plays an important role in lipid metabolism and signal transduction (16–18). A study demonstrated that DHCR24 knockdown decreased caveolin-1 protein expression (19), indicating that DHCR24 might modulate it. In contrast, caveolin-1 is required to bind integrins to the ERK pathway and promote cell-cycle progression (20,21), which is linked to senescence. Caveolin-1 suppression also inhibited the activation of the ERK signaling pathway (22). In addition, some studies have demonstrated that caveolin-1 can prevent cell senescence by inhibiting reactive oxygen species (ROS) production (18,23,24). Therefore, we hypothesized that decreased caveolin-1 due to DHCR24 deficiency might induce ECs senescence through ERK signaling during senescence. The present study aimed to investigate the effects of DHCR24 deficiency on ECs senescence and endothelial dysfunction in endothelial-specific DHCR24 knockout mice and endothelial senescent cell models and explored the potential mechanisms in cultured ECs.

Materials and Methods

Cell Culture

Human umbilical vein endothelial cells (HUVECs) were freshly isolated from 3 to 5 human umbilical cord veins, as previously described (25). The umbilical cord was collected from the donor (age 25–30) with informed consent, as approved by the Human Experimentation Ethics Committee of Tongji Hospital, Huazhong University of Science and Technology (TJ-IRB20230419). Isolated HUVECs were resuspended in medium 199 supplemented with 10% fetal bovine serum (FBS; Biological Industries, Israel) and 2% low serum growth supplement (Gibco, USA) before being inoculated in

culture flutes (T25). Cells were cultured in a constant temperature incubator at 37°C with a 5% CO₂ atmosphere and subcultured with 0.05% trypsin-EDTA (Gibco) at 80% confluence. Replicative senescence model was established by consecutively passaging the young HUVECs until the cell proliferation was nearly arrested. Young and old HUVECs used in the experiments were from passage 5 (P5) and passage 13 (P13), respectively.

Pulmonary Microvascular Endothelial Cells Isolation and Culture

Primary pulmonary microvascular endothelial cells (PMVECs) were isolated from lung tissues in *DHCR24 flox/flox-Tie2Cre⁻* mice and *DHCR24 flox/flox-Tie2Cre⁺* mice, as previously described (26). Hundred microliter of sheep anti-rat IgG Dynabeads (Thermo Fisher, USA) were mixed with 5 μ g anti-mouse PECAM-1 (BD Pharmingen, USA). The beads and antibody were incubated overnight at 4°C. Fresh mouse lung tissue was isolated and washed with PBS, before being transferred to cryopreservation tubes and cut into pieces with sterile scissors. The lung tissue fragments were digested with collagenase for 45 minutes in a 37°C shaker. The cells were filtered through sterile 70- μ m nylon mesh and washed twice with 0.1% bovine serum albumin (BSA; Solarbio, China).

To allow binding to cells, 30 μ L of coated Dynabeads were added to cells and incubated for 25 minutes at room temperature. All bead-bound cells were resuspended in DMEM containing 20% FBS before plating and purified with Anti-ICAM-2 (BD Pharmingen) antibody-conjugated Dynabeads when the cell confluences reached 70% to 80% or above.

Senescence-Associated β -Galactosidase Activity Assay

Senescence-associated β -galactosidase (SA- β -gal) staining was examined using a Senescence β -Galactosidase Staining Kit (Beyotime, China) according to the manufacturer's protocol. Briefly, cells were seeded and grown in 12-well plates. Whether stimulated or not, when the cells confluences reached about 60%, they were washed once with PBS, fixed with fixing solution for 15 minutes at room temperature, and then incubated in a new staining solution without CO₂ overnight at 37°C. The cells were examined using an inverted ordinary light microscope (OLYMPUS CKX41). Image J was used to count blue-stained cells and total cells. The percentage of β -galactosidase positive cells was calculated.

Cell Proliferation Assay

Cell proliferation was measured by Edu staining using an iClick™ Edu Andy Flour 488/555 Imaging Kit (Wuhan ABP-Biosciences Co., Ltd, China), according to the manufacturer's instructions. Briefly, cells seeded in 12-well plates were grown to about 70% before being incubated with 10 μ M Edu for 2 hours. The cells were washed once with PBS, fixed with 3.7% formaldehyde PBS for 15 minutes, and then treated with 0.5% Triton X-100 permeable membrane for 20 minutes. After washing, they were incubated for 30 minutes away from light with an iClick reaction buffer at room temperature. Cells were then counterstained with 5 μ g/mL Hoechst 33342 and examined using an inverted fluorescence microscope (OLYMPUS IX71). Edu-positive and DAPI-positive nuclei were counted automatically using Image J.

Western Blot

Total protein was extracted using RIPA lysis (Boster, China) buffer containing protease and phosphatase inhibitors. The BCA Protein Assay Kit (Boster) was used to determine protein concentrations. Equal quantities of proteins were separated by electrophoresis on sodium dodecyl sulfate-polyacrylamide gels and transferred to polypropylene difluoride membranes (Millipore, USA). At room temperature, the membranes were blocked in 5% nonfat milk for 1 hour. Primary antibodies against GADPH (#10494-1-AP, 1:4 000, Proteintech, China), DHCR24 (#2033S, 1:1 000, Cell Signaling Technology, USA), SIRT1 (#8469S, 1:1 000, Cell Signaling Technology), P16 (#ab51243, 1:1 000, Abcam, UK), caveolin-1 (#A1555, 1:1 000, ABclonal, China), p-ERK (#4370T 1:1 000, Cell Signaling Technology), ERK (#4695T 1:1 000, Cell Signaling Technology), p-c-myc (#AP0989, 1:1 000, ABclonal), c-myc (#A19032, 1:1 000, ABclonal), and eNOS (#32027S, 1:1 000, Cell Signaling Technology) were incubated at 4°C overnight. The membranes were then incubated for 1 hour at room temperature with horseradish peroxidase (HRP)-conjugated secondary antibodies (1:5 000; Promotor, China). Finally, chemiluminescence was detected with an enhanced chemiluminescence kit (Beyotime).

siRNA Interference

The DHCR24 siRNA-targeting sequence was 5'-GCTG AATAGCATTGGCAAT-3', designed and synthesized by Ribobo (Guang Zhou, China). The nontargeting siRNA (5'-TTCTCCGAACGTGTCACGTdTdT-3') that served as a negative control was obtained similarly. Transfection was performed with 30 nmol/L siRNA using lipo3000 transfection reagent (Invitrogen). When HUVECs (P5) density reached 50%–70%, lipo3000 transfection reagent (Invitrogen) and siRNA were added to the starvation medium containing 2% FBS. Furthermore, the complete medium containing 10% FBS was replaced 6 hours later. Gene silencing efficiency was assessed by q-PCR and western blot.

Lentiviral Overexpression of DHCR24

Lentiviral production was purchased from GeneChem (Shanghai, China). The lentivirus for DHCR24 overexpression was named "OE-DHCR24," whereas the control lentivirus was named "CON." HUVECs (P13) were transfected with the lentiviral using the manufacturer's protocol. The vector name is "GV492," and the element order is "UB-MCS-3FLAG-CBH-gcGFP-IREs-puromycin." A mixture of virus diluent (MOI = 100), HitansG, and complete medium was allowed to stand for 10 minutes before adding to HUVECs. Notably, a complete medium should be replaced 8 hours after transfection, and puromycin at 0.5 µg/mL could be used for screening 72 hours after transfection. The efficiency of gene overexpression was confirmed using q-PCR and western blot.

Measurement of Intracellular NO

Nitric oxide release was measured using 3-amino,4-aminomethyl-2',7'-difluorescein, diacetate (DAF-FM DA; Beyotime) according to the standard protocol. The cells were seeded on confocal small dishes and washed thrice with calcium- and magnesium-containing Hank's balanced salt solution (HBSS). The cells were then incubated for 20 minutes at 37°C with DAF-FM DA (5 mM). After 3 more HBSS

washes, the fluorescence intensity was measured using a Nikon C2 confocal microscope.

Measurement of Intracellular ROS

The fluorescent probe dihydroethidium (MCE, China) was used to assess intracellular ROS generation. HUVECs were washed with M199 and incubated in a dark chamber for 30 minutes with dihydroethidium (10 µmol/L) at 37°C. After washing thrice with M199, the fluorescent signal intensity was measured using an inversion fluorescence microscope.

Cell Tube Formation

Matrigel tube formation assay was used to determine HUVECs tube formation capacity. Matrigel (Corning, USA) was thawed at 4°C overnight. The liquid Matrigel was spread into 96-well plates (50 µL per well) and incubated in a 5% CO₂ incubator at 37°C for 40 minutes. Cell suspensions were counted using a Cellometer-Mini Automatic Cell Counter (Nexcelom Bioscience, Lawrence, MA, USA). HUVECs (5 × 10³ per well) were seeded on the Matrigel-coated plates and incubated for 6 hours. The network formation in Matrigel was observed using an inverted light microscope. The Image J software plugin "Angiogenesis Analyzer" quantified the extent of tube formation before statistical analysis.

Cell Migration Assay

A transwell chamber (Corning) with a pore size of 8.0 µm was used to measure migration. In brief, 5 × 10⁴ cells were seeded in 200 µL serum-free medium in the upper chamber. A complete medium (600 µL) containing 10% FBS was placed in the bottom chamber. Cells were cultured for 24 hours to pass through the polycarbonate to the lower surface of the upper chamber. The upper chamber was fixed with 4% paraformaldehyde, washed thrice with PBS, and stained for 15 minutes with crystal violet solution. Cells that did not migrate were removed with a cotton swab, and the membrane was imaged under an inverted light microscope. Bound crystal violet was dissolved in 95% ethanol solution for quantification, and the absorbance at 570 nm was measured.

Animals

Vascular endothelium-specific *DHCR24* knockout mice were developed in a C57BL/6 background using standard Cre-LoxP-based gene targeting strategies. Mice carrying loxP-flanked *DHCR24* alleles (*DHCR24*^{flox/flox}) and *Tie2*-Cre transgenics were interbred. *DHCR24*^{flox/flox} mice and *Tie2*-Cre mice were purchased from Gempharmatech Co., Ltd (Jiangsu, Nanjing, China). In brief, according to the structure and exon size of the *DHCR24* gene, exon3 of the *DHCR24* transcript could be conditionally removed. Cas9 mRNA and gRNA (CAGGGACCAGAATACTGCCC) were cloned into the pX458 plasmid vector for transcription in vitro. Then they were injected into mouse fertilized eggs for homologous recombination. The F0 mice verified by PCR and sequencing were backcrossed with C57BL/6J mice to obtain F1 mice (*DHCR24*^{flox/flox}). The flox region of *DHCR24*^{flox/flox} mouse was eliminated through crossing with a mouse expressing endothelium-specific Cre recombinase. The *DHCR24* deletion in vascular endothelium was confirmed by PCR of genomic DNA isolated from mouse tails. Mice were kept in a pathogen-free environment with constant room temperature (22 ± 2°C) and humidity (40%–60%). They were fed a standard mouse diet and water ad libitum with a 12:12-h light/

dark cycle. After 10 months of feeding, mice were divided into 2 groups based on their genotypes: *DHCR24 flox/flox-Tie2Cre⁻* and *DHCR24 flox/flox-Tie2Cre⁺*. Male C57BL/6 mice at different ages (3 and 14 months) were purchased from Vital River Laboratories. Animals were anesthetized with an intraperitoneal injection of 1% sodium pentobarbital (30 mg/kg) at the time of sacrifice. All animal procedures were approved by the Laboratory Animal Welfare and Ethics Committee of Tongji Hospital, Huazhong University of Science and Technology (TJH-202108010).

Assessment of Vascular Function

Measurement of blood pressure

Mouse blood pressure was measured in vivo and vascular ring tension was measured in vitro to assess vascular function. Noninvasive blood pressure was measured by using a CODA monitor noninvasive blood pressure system (Kent Scientific Corporation, Torrington, CT, USA). Awake mice were placed on a heated panel for 10 minutes before being placed in a fixer to acclimatize to their environment. The mouse tail was occluded by a tubular cuff attached to the tail-cuff device. Each recording session included 15 inflation and deflation cycles and 5 initial “acclimation” cycles. Take at least 5 consecutive blood pressure readings and calculate the average.

Measurement of vascular reactivity

The measurement of vascular reactivity in the mouse thoracic aorta has been previously described (27). In brief, an intact thoracic aortic ring (2 mm) was mounted on an isometric wire myograph (DMT620M, ADInstruments, Australia) filled with physiological saline solution aerated with 95% O₂ and 5% CO₂. The aortic ring was gradually stretched to an optimal baseline tension of 5 mN while equilibrating for 60 minutes. The aortic ring was constricted twice with 60 mM KCl, and the maximum amplitude of the contractile response was similar. To assess endothelium-dependent vasodilatation, relaxation was achieved by cumulative addition of acetylcholine (ACh, 10⁻⁹ to 10⁻³ M, A6625, MCE) at maximum amplitude.

Immunofluorescence

The paraffin-embedded sections of the thoracic aorta were stained by immunofluorescence. In brief, the sections were dewaxed with xylene and gradient alcohol before being repaired for 2 minutes at high temperature and pressure with EDTA antigen retrieval solution (pH 9.0). The sections were washed thrice with TBST buffer and blocked with 3% H₂O₂ at room temperature for 30 minutes. After being immersed in distilled water, the sections were incubated with 10% goat serum at 37°C for 30 minutes. The serum was discarded, the primary antibody anti-CD31 (#ab182981, 1:200, Abcam) was added and left at 4°C overnight. After washing with TBST, the secondary antibody Goat Anti-Rabbit IgG H&L (HRP; #ab2057188, 1:4 000, Abcam) was incubated at 37°C for 45 minutes. The working solution of iFluor 488 tyramide (#11060, 1:300, aatbio, USA) was then incubated at room temperature for 10 minutes. After elution and blocking again, primary antibodies against DHCR24 (#GTX103712, 1:300, GeneTex), P16 (#ab51243, 1:200, Abcam), and secondary antibodies were incubated and stained with Cy5-Tyramide (#11066, 1:400, aatbio). The nucleus was stained, and the sections were sealed with an anti-British photoquenched tablet

binder (containing DAPI). The sections were visualized and imaged using fluorescence confocal microscopy (Nikon C2).

Statistical Analysis

All statistical analyses were performed using GraphPad Prism 9.0. The data were presented as means ± standard deviation (SD) and were analyzed by Student's *t* test, 1-way ANOVA or 2-way ANOVA. Each experiment was repeated thrice. Statistical differences were considered significant at *p* values < .05.

Results

DHCR24 Was Decreased in Senescent HUVECs and Aged Blood Vessels

We used a replicated senescence cell model and aged mice to investigate how DHCR24 expression changes with age. Senescent cells exhibit a positive staining for SA-β-gal, increased senescence marker P16 expression, and decreased proliferation and SIRT1 expression (10,28–30). The old group (P13) had more SA-β-gal-stained cells (Figure 1A and B) and lower cell proliferation capacity (Figure 1C and D), suggesting a successful replicative senescence cell model. Furthermore, the senescence marker P16 was increased and SIRT1 was

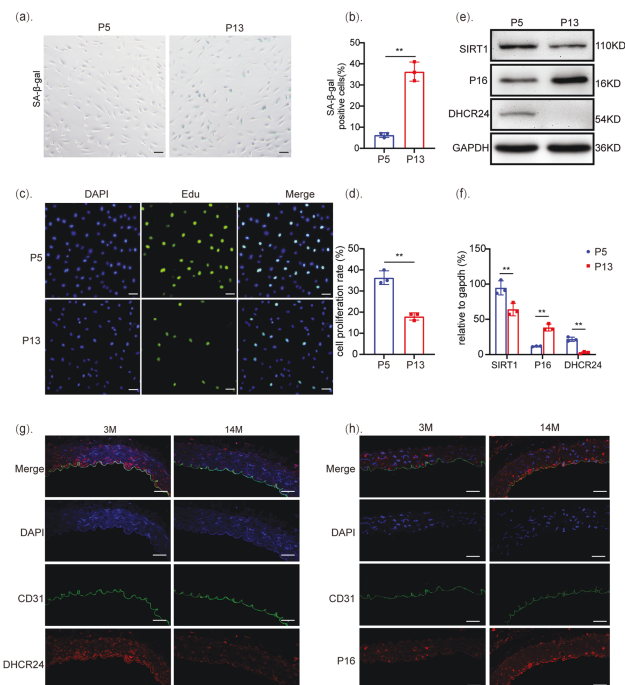


Figure 1. Decreased DHCR24 expression in senescent human umbilical vein endothelial cells (HUVECs) and aged blood vessels. (A, B) Senescence-associated-β-galactosidase (SA-β-gal) staining of young (P5) and old (P13) HUVECs. Scale bar: 100 μm. Statistical significance was determined using Student's *t* test. (C, D) Edu for young (P5) and old (P13) HUVECs proliferation. Scale bar: 100 μm. Statistical significance was analyzed using Student's *t* test. (E, F) Verification of DHCR24, P16, and SIRT1 expression in young (P5) versus old (P13) by western blot analysis. The statistical significance was measured using 2-way ANOVA. (G) Immunofluorescent staining for DHCR24 (red), CD31 (green), and nuclei (blue) in paraffin-embedded aorta tissue sections from young (3 months) and aged (14 months) mice. Scale bar: 50 μm. (H) Expression of p16 (red) and CD31 (green) in paraffin-embedded aorta tissue sections from young (3 months) and aged (14 months) mice. Hoechst stained nuclei (blue). Scale bar: 50 μm. *n* = 3. The values are presented as mean ± SD. **p* < .05, ***p* < .01.

decreased in the old group (P13) compared to the young group (P5; Figure 1E and F). We found that the DHCR24 protein expression level was lower in the old HUVECs (P13; Figure 1E and F). In addition, we used immunofluorescence staining to examine DHCR24 in the thoracic aorta of 3-month-old and 14-month-old mice. The aortic DHCR24 and P16 protein signals are inversely related to age (Figure 1G and H). The findings indicated that DHCR24 expression is down-regulated with age.

DHCR24 $flox/flox$ -Tie2Cre $^+$ Mice Present ECs Senescence and Endothelial Dysfunction

To determine whether the deficiency of DHCR24 contributes to endothelial senescence and dysfunction, we established a vascular endothelium-specific DHCR24 knockout mouse model using CRISPR/Cas9 technology. There was no difference in body weight between DHCR24 $flox/flox$ -Tie2Cre $^-$ and DHCR24 $flox/flox$ -Tie2Cre $^+$ mice, and no defect was observed in DHCR24 $flox/flox$ -Tie2Cre $^+$ mice (Figure 2A). We then performed an ex vivo vascular ring tension assay and noninvasive blood pressure measurement to assess vascular endothelium-dependent vasodilatation function and blood pressure. The vasodilation of aorta rings in response to Ach was significantly reduced in DHCR24 $flox/flox$ -Tie2Cre $^+$ mice (Figure 2B). DHCR24 $flox/flox$ -Tie2Cre $^+$ had higher systolic blood pressure than DHCR24 $flox/flox$ -Tie2Cre $^-$ mice (Figure 2C). Endothelium-specific deletion of DHCR24 was confirmed by genotype identification (Supplementary Figure S1A). We also confirmed DHCR24 expression in the aortas of DHCR24 $flox/flox$ -Tie2Cre $^+$ mice (Figure 2D). Western blot analysis of pulmonary microvascular endothelial cells (PMVECs) revealed that SIRT1 decreased with DHCR24 deficiency, and the senescence marker P16 increased (Figure 2E and F). This is consistent with the P16 protein signals detected by immunofluorescence staining of paraffin-embedded aorta tissue sections from DHCR24 $flox/flox$ -Tie2Cre $^-$ mice and DHCR24 $flox/flox$ -Tie2Cre $^+$ mice (Figure 2G). Meanwhile, the PMVECs from DHCR24 $flox/flox$ -Tie2Cre $^+$ mice had reduced proliferative capacity (Figure 2H and I), and increased SASP mRNA including MMP3, MMP10, MMP13, PAI-1, PAI-2, CCL8, and so on (Supplementary Figure S1B). Endothelial nitric oxide synthase (eNOS) produces nitric oxide (NO), which regulates systemic blood pressure and vasodilator function (31,32). Here, we showed that DHCR24 $flox/flox$ -Tie2Cre $^+$ mice PMVECs had lower eNOS and NO than controls (Figure 2E, F, J, and K). These findings suggest that a deficiency of vascular endothelium-specific DHCR24 causes vascular aging and endothelial dysfunction. DHCR24 may be protective in senescent ECs.

DHCR24 Protects Against ECs Senescence and Endothelial Dysfunction

Our in vivo studies revealed that DHCR24 is important in ECs senescence and endothelial dysfunction. Furthermore, we investigated the mechanism of DHCR24 in vitro. The DHCR24 was knocked down with siRNA in young HUVECs (P5), and its expression was reduced significantly than the NC group (Figure 3A and B). The senescence marker P16 (Figure 3A and B), SA- β -gal activity (Figure 3C and D), and SASP mRNA levels (including MMP3, MMP10, MMP13, PAI-1, etc.; Supplementary Figure S2A) were increased in DHCR24-knockdown cells compared to the NC group. In

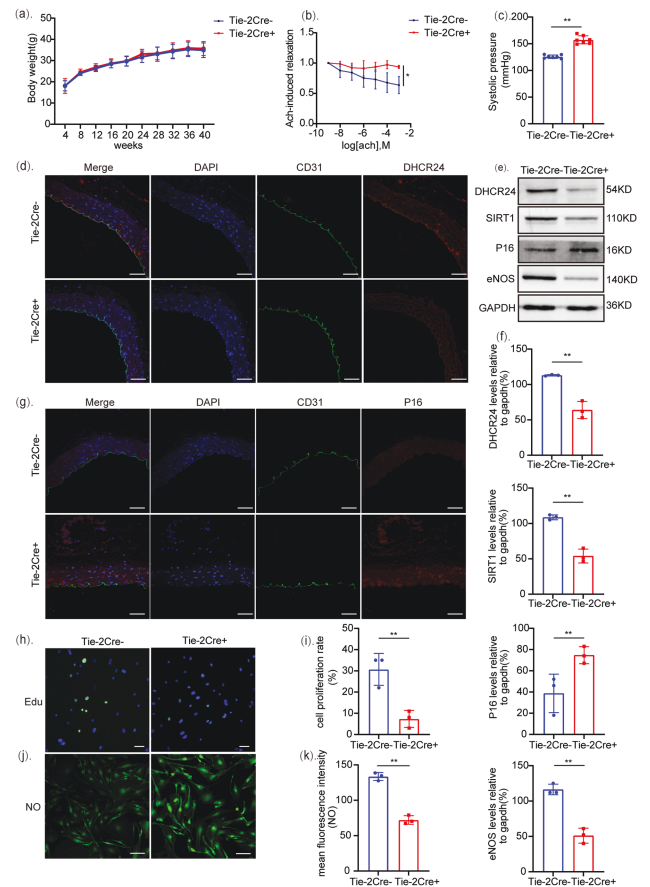


Figure 2. Endothelium-specific DHCR24 knockout mice have endothelial cells (ECs) senescence and endothelial dysfunction. (A) Body weight of DHCR24 $flox/flox$ -Tie2Cre $^-$ and DHCR24 $flox/flox$ -Tie2Cre $^+$ mice. (B) Acetylcholine (Ach)-induced endothelium-dependent vascular relaxation in the aorta rings of DHCR24 $flox/flox$ -Tie2Cre $^-$ mice and DHCR24 $flox/flox$ -Tie2Cre $^+$ mice at 10 months. The cumulative concentration response curves were recorded, and statistical significance was determined using Student's *t* test. (C) Systolic blood pressure in DHCR24 $flox/flox$ -Tie2Cre $^-$ mice and DHCR24 $flox/flox$ -Tie2Cre $^+$ mice. (D) Immunofluorescent staining for DHCR24 (red), CD31 (green), and nuclei (blue) in paraffin-embedded aortic tissue sections from DHCR24 $flox/flox$ -Tie2Cre $^-$ and DHCR24 $flox/flox$ -Tie2Cre $^+$ mice. Scale bar = 50 μ m. (E, F) Western blot analysis of DHCR24, SIRT1, P16, and eNOS expression in the PMVECs from DHCR24 $flox/flox$ -Tie2Cre $^-$ mice and DHCR24 $flox/flox$ -Tie2Cre $^+$ mice. (G) Expression of P16 (red) and CD31 (green) in paraffin-embedded aorta tissue sections from DHCR24 $flox/flox$ -Tie2Cre $^-$ and DHCR24 $flox/flox$ -Tie2Cre $^+$ mice. Nuclei (blue) stained by Hoechst. Scale bar: 50 μ m. (H, I) Edu for the cell proliferation of PMVECs from DHCR24 $flox/flox$ -Tie2Cre $^-$ mice and DHCR24 $flox/flox$ -Tie2Cre $^+$ mice. Scale bar = 100 μ m. (J, K) Fluorescence images of intracellular nitric oxide (NO) of pulmonary microvascular endothelial cells (PMVECs) stained with 3-amino,4-aminomethyl-2',7'-difluorescein, diacetate (DAF-FM DA). $n \geq 3$. The values are presented as mean \pm SD. * $p < .05$, ** $p < .01$.

contrast, the senescence-associated gene SIRT1 (Figure 3A and B) and cell proliferation capacity (Figure 3E and F) were decreased. Furthermore, the reduction of eNOS (Supplementary Figure S2B and C) and NO (Figure 3G and H) levels in DHCR24-knockdown cells was confirmed. We also investigated the function of HUVECs through a migration assay and a tube formation assay. DHCR24 knockdown impaired endothelial migration (Supplementary Figure S2D and E). The NC group cells appeared elongated and tubular, whereas DHCR24-knockdown cell tube formation was inhibited,

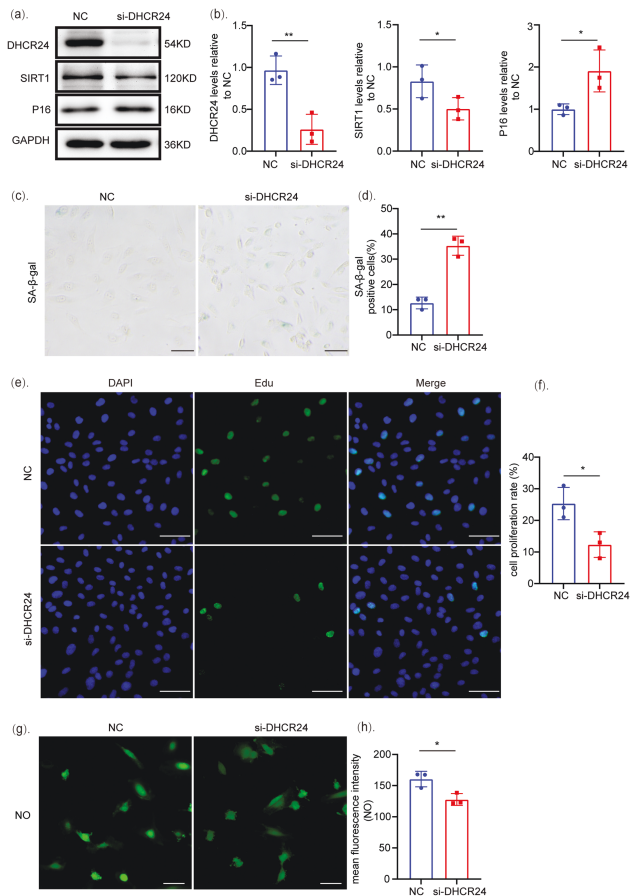


Figure 3. Increased endothelial cell senescence by DHCR24 gene knockdown. (A, B) DHCR24, SIRT1, and P16 expression in young human umbilical vein endothelial cells (HUVECs) (P5) treated with siRNA targeting the human DHCR24. (C, D) SA-β-gal staining in young HUVECs (P5) transfected with siDHCR24 and quantitative data for SA-β-gal-positive cells. Scale bar: 100 μm. (E, F) Edu for DHCR24-knockdown HUVECs proliferation. Scale bar: 100 μm. (G, H) Fluorescence images of intracellular NO of young HUVECs (P5) transfected with siDHCR24 staining with 3-amino,4-aminomethyl-2',7'-difluorescein, diacetate (DAF-FM DA). Scale bar: 50 μm. The Student's *t* test was used to determine the statistical significance. *n* = 3. The values are presented as mean ± *SD*. **p* < .05, ***p* < .01.

resulting in an incomplete or sparse tubular network (Supplementary Figure S2F and G).

To investigate the protective role of DHCR24, we analyzed the effects of lentivirus-induced DHCR24 overexpression in senescent HUVECs (P13). Similarly, detecting DHCR24 protein expression was used to assess the overexpression efficiency (Supplementary Figure S3A and B). The senescence marker P16 (Supplementary Figure S3A and B), SA-β-gal activity (Supplementary Figure S3C and D) and SASP mRNA levels (including MMP3, MMP10, MMP13, PAI-1, etc.; Supplementary Figure S3O) were significantly reduced in DHCR24-overexpression cells than in the CON group. The senescence-associated gene SIRT1 (Supplementary Figure S3A and B) and cell proliferation capacity (Supplementary Figure S3E and F) were recovered in the senescent cells. DHCR24-overexpression cells produced more eNOS (Supplementary Figure S3G and H) and NO (Supplementary Figure S3I and J) than the CON group. DHCR24 overexpression improved cell migration compared to senescent cells from the CON group (Supplementary Figure S3K and L). Similarly, DHCR24

overexpression restored tubule formation and increased the total branching length and number of junctions in senescent cells (Supplementary Figure S3M and N). These findings strongly suggest that DHCR24 protects ECs from senescence and dysfunction.

Caveolin-1/ERK is Critical to Developing DHCR24 Deficiency-Induced ECs Senescence and Dysfunction

Caveolin-1 is an indispensable protein of caveolae, which are sphingolipids and cholesterol-rich invaginated microstructures of the plasma membrane (16). We investigated whether DHCR24 affects caveolin-1 and downstream signaling molecules expression because DHCR24 deficiency restricts cholesterol synthesis (33). Compared to the negative control group, DHCR24 knockdown significantly reduces caveolin-1, decreased the phosphorylation of ERK and its downstream molecule c-myc in young HUVECs (P5; Figure 4A and B). In contrast, we identified that after DHCR24 overexpression in old HUVECs (P13), the above levels are higher than in the senescence control group (Figure 4C and D). In addition, inhibiting ERK signaling using U0126 increased the P16 expression (Figure 4E and F) and SA-β-gal activity (Figure 4G and H) while attenuating cell proliferation (Figure 4I and J). ROS production is a determinant of ECs senescence and dysfunction, so the ERK/ROS pathway may be involved in this process. Therefore, dihydroethidium staining was used to assess ROS production. DHCR24-knockdown cells fluoresced more red than control cells (Supplementary Figure S4A), indicating higher intracellular ROS levels. The high level of ROS was indirectly confirmed by MDA, a marker of lipid peroxidation (Supplementary Figure S4B), 8-OHdG, a marker of DNA oxidative damage (Supplementary Figure S4C), and protein carbonyl content, a marker of protein oxidative damage (Supplementary Figure S4D). However, DHCR24-overexpression cells demonstrated the opposite effects (Supplementary Figure S4E–H). These findings suggest that caveolin-1/ERK signaling is involved in the DHCR24 depletion-induced ECs senescence and dysfunction.

Desmosterol Accumulation in DHCR24 Deficiency Induces ECs Senescence and Endothelial Dysfunction

DHCR24 catalyzes cholesterol synthesis via Kandutsch–Russell pathway and Bloch pathway, with lanosterol and desmosterol as precursors, respectively, and mutations in DHCR24 result in high desmosterol levels (34). Consistently, the cholesterol and desmosterol in DHCR24-knockdown cells reduced and increased, respectively, compared to the NC group (Figure 5A). Similar changes in cholesterol and desmosterol were observed in old HUVECs (P13; Figure 5B). However, there was no significant difference in lanosterol (Supplementary Figure S5A and B). To investigate whether DHCR24 deficiency-induced ECs senescence is mediated by desmosterol accumulation, we treated HUVECs with desmosterol. We found that senescence marker P16 (Figure 5C and D) and SA-β-gal activity (Figure 5E and F) increased with desmosterol concentration. The senescence-associated gene SIRT1 (Figure 5C and D) and cell proliferation capacity (Figure 5G and H) were decreased with increasing desmosterol concentrations.

Next, we examined whether caveolin-1/ERK is a desmosterol target. Western blot analysis revealed that the

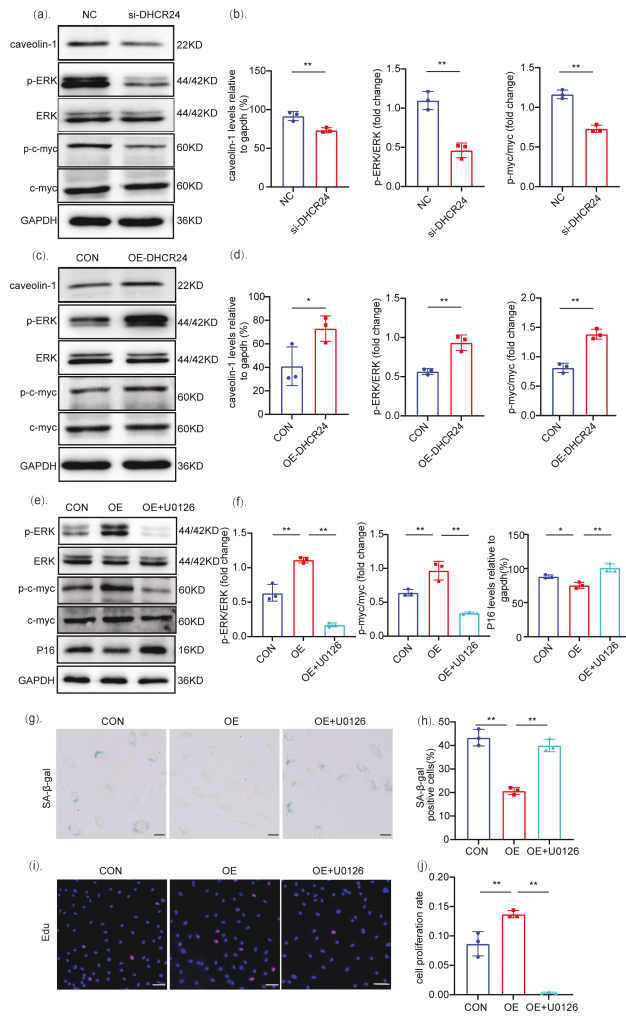


Figure 4. Caveolin-1/ERK is critical to developing DHCR24 deficiency-induced endothelial cells (ECs) senescence and dysfunction. (A, B) Western blot analysis of caveolin-1 and p-ERK expression in young human umbilical vein endothelial cells (HUVECs) (P5) transfected with siDHCR24. (C, D) Western blot analysis of caveolin-1 and p-ERK expression in old HUVECs (P13) transfected with DHCR24 lentivirus. The statistical significance was measured using Student's *t* test. (E, F) Western blot analysis of p-ERK, p-myc, and P16 expression in HUVECs transfected with the DHCR24 lentivirus and then treated with the ERK inhibitor U0126. (G, H) SA-β-gal staining in HUVECs transfected with the DHCR24 lentivirus and then treated with the ERK inhibitor U0126. Percentage of SA-β-gal-positive cells was calculated. Means are compared using 1-way ANOVA. Scale bar: 50 μm. (I, J) Edu for cell proliferation of HUVECs transfected with DHCR24 lentivirus and followed by ERK inhibitor U0126 treatment. Means are compared using 1-way ANOVA. Scale bar: 100 μm. *n* = 3. The values are presented as mean ± *SD*. **p* < .05, ***p* < .01.

caveolin-1, ERK, and c-myc phosphorylation levels decreased with desmosterol concentration (Figure 5C and D). Similarly, we investigated whether desmosterol accumulation affects endothelial functions. We observed that eNOS and NO levels decreased with an increase in desmosterol concentration (Figure 5C, D, M, and N), whereas intracellular ROS (Figure 5I and J) and 8-OHdG (Figure 5K and L) increased, doing the opposite. These findings indicate that desmosterol accumulation may contribute to endothelial senescence and dysfunction caused by DHCR24 depletion.

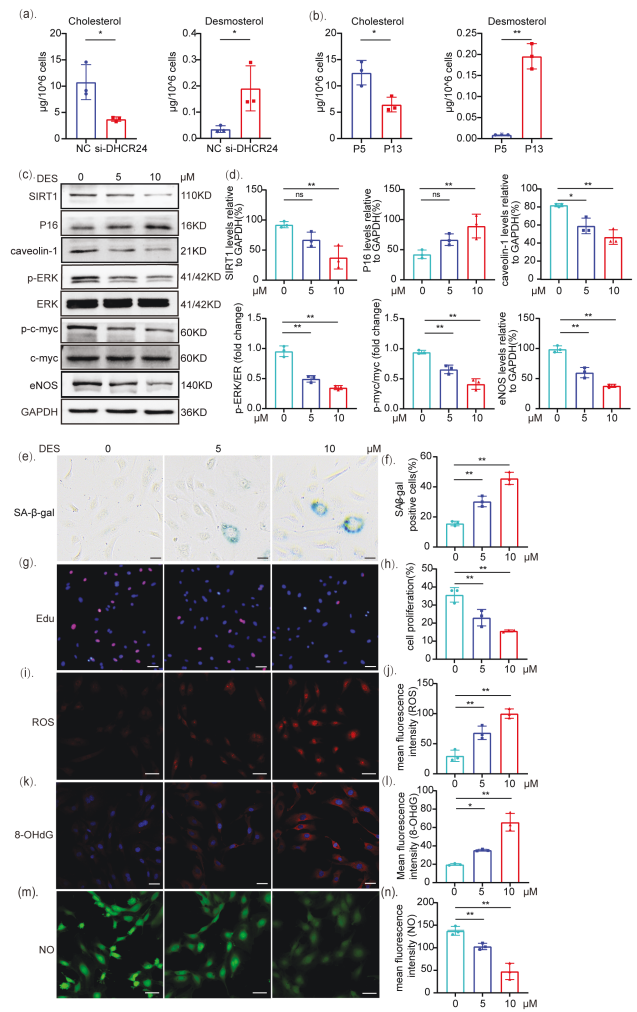


Figure 5. Desmosterol accumulation in DHCR24 deficiency induces endothelial cells (ECs) senescence. (A, B) Cholesterol and desmosterol levels were measured by GC-MS in human umbilical vein endothelial cells (HUVECs). (C, D) Western blot analysis of SIRT1, P16, eNOS, caveolin-1, p-ERK, and p-myc expression in desmosterol-treated HUVECs (P5). (E, F) Senescence-associated-β-galactosidase (SA-β-gal) staining in desmosterol-transfected HUVECs (P5) and quantitative data for SA-β-gal-positive cells. Scale bar: 50 μm. (G, H) Edu for the cell proliferation of desmosterol-transfected HUVECs (P5) and quantitative data. Scale bar: 100 μm. (I–N) Fluorescence images of intracellular reactive oxygen species (ROS), 8-OHdG, and nitric oxide (NO) of desmosterol-treated HUVECs (P5). Scale bar: 50 μm. Statistical significance was determined using 1-way ANOVA. *n* = 3. The values are presented as mean ± *SD*. **p* < .05, ***p* < .01.

Discussion

The present study demonstrates that the DHCR24 expression decreased chronologically and promotes ECs senescence and endothelial dysfunction through the caveolin-1/ERK signaling axis. Furthermore, desmosterol accumulation caused by DHCR24 deficiency may significantly contribute to the pathological process.

Vascular ECs senescence is important in vascular aging, which is closely related to the occurrence and progression of age-related diseases (6,8,35). The findings of the present study confirmed DHCR24 down-regulation in senescent cells and aortic endothelium. Senescent ECs were also found in vessels isolated from the dorsolateral prefrontal cortex of AD

patients (35). Greeve et al. demonstrated that DHCR24 was down-regulated in the susceptible brain area of AD (34,36). However, previous studies have failed to provide significant evidence for link between DHCR24 and ECs senescence. The relationship between DHCR24 in senescent ECs and other age-related diseases remains unknown. Regardless, DHCR24 down-regulation in senescent ECs may play an important role in age-related disease. Exploring the mechanism of DHCR24 in ECs senescence is expected to find a therapeutic target for age-related diseases.

Endothelial cells senescence is critical for vascular age-related endothelial dysfunction, such as vascular tone dysregulation, arterial stiffness, and systolic hypertension (8). The present study demonstrated that *DHCR24^{flox/flox}-Tie2^{Cre}* mice had higher systolic blood pressure and an impaired diastolic response of the aortic ring to Ach. NO is responsible for maintaining vasodilator function (5). Similarly, we identified that PMVECs from *DHCR24^{flox/flox}-Tie2^{Cre}* mice had down-regulated NO levels. We also found that PMVECs from *DHCR24^{flox/flox}-Tie2^{Cre}* mice exhibit distinct senescent features, such as reduced proliferation potential, decreased expression of senescence-related protein SIRT1, and increased expression of cyclin-dependent kinase inhibitory protein P16.

Moreover, the knocking down DHCR24 in young HUVECs resulted in phenotypes similar to the PMVECs senescence. Furthermore, DHCR24 deficiency impaired tubule formation, migration, and NO levels. While overexpression of DHCR24 in the senescent HUVECs recaptures these senescence-associated alterations. The classically recognized endothelial function of cultured cells includes cell migration, proliferation, angiogenesis, and eNOS-derived NO bioavailability. Therefore, DHCR24 plays a key role in improving ECs senescence and dysfunction. DHCR24 could be a promising therapeutic target for age-related diseases.

Caveolin-1 is a signature structural protein of caveolae that is rich in cholesterol (16,17). DHCR24 is also involved in cholesterol biosynthesis. Therefore, the expression level of caveolin-1 is influenced by the content or activity of DHCR24. The findings revealed that DHCR24 deficiency decreased caveolin-1 expression, which is consistent with the results of Xiuli Lu (19). Studies revealed that the caveolin-1/ERK signaling axis plays an important role in cell proliferation (21,37–40), a key feature of senescent cells. The results of the present study indicate that DHCR24 deficiency attenuated ERK phosphorylation, whereas DHCR24 overexpression reversed these effects. Moreover, U0126 treatment increased SA- β -gal activity while reducing proliferation in DHCR24-overexpressing cells. Thus, the caveolin-1/ERK pathway was involved in DHCR24 deficiency-induced senescence.

Traditionally, oxidative stress induced by ROS accumulation has been identified as a driver of cell senescence. In this study, we observed that DHCR24 knockdown in young cells increased ROS production, whereas overexpression of DHCR24 in senescent cells reduced it. ERK phosphorylation induces catalase activity and decreases ROS levels, such that ERK signaling activation are inversely related to ROS (41,42). Therefore, ECs senescence caused by DHCR24 deficiency via the caveolin-1/ERK pathway may be related to oxidative stress. This may provide additional avenues to explain the role of DHCR24 in scavenging ROS and protecting against oxidative stress (12). ROS production increased

significantly, with a decrease in eNOS and NO levels (43,44). Similarly, we identified that DHCR24 deficiency significantly inhibited eNOS and NO levels, whereas DHCR24 overexpression produced the opposite results. Endothelial dysfunction induced by DHCR24 deficiency may be due to oxidative stress. Therefore, these findings imply that the caveolin/ERK signaling axis is a key mechanism by which DHCR24 regulates endothelial senescence and dysfunction.

Previous studies have shown that DHCR24 acts as the final step reaction enzyme in the cholesterol synthesis from desmosterol and that its deletion induces desmosterol accumulation (19,44,45), consistent with our findings. We treated HUVECs with desmosterol to explore whether the endothelial senescence and dysfunction caused by DHCR24 deficiency were associated with increased desmosterol. The results revealed that desmosterol increased the SA- β -gal activity while inhibiting cell proliferation. Previous studies have demonstrated that the replacing of cholesterol with desmosterol does not preserve the caveolae integrity (19), but the mechanism is unknown. In our study, it was first found that desmosterol inhibited caveolin-1 expression.

Meanwhile, desmosterol treatment inhibited ERK signaling, increased ROS production, and inhibited eNOS/NO production, implying that desmosterol accumulation is one of the causes of DHCR24 deficiency-induced ECs senescence and endothelial dysfunction. These findings suggest that DHCR24 plays an important role in vascular endothelial senescence and dysfunction. This is essential for discovering novel therapeutic and preventive strategies for age-related vascular diseases.

Although cholesterol is obtained in mammalian cells mainly through 2 pathways: exogenous uptake and endogenous synthesis (46), it has been shown that the endogenous synthesis of DHCR24 is important for maintaining cholesterol homeostasis in plasma (47). This suggests that the endogenous cholesterol synthesis pathway is essential for maintaining cholesterol homeostasis in plasma. Furthermore, we show that DHCR24 in ECs regulates cellular cholesterol/desmosterol expression and is involved in cell senescence. Given the role of cholesterol in normal eukaryotic cell membrane structure and function, DHCR24 may regulate senescence in other cell types. Moreover, endothelial cell senescence is associated with systemic aging (48), and DHCR24 in ECs may play an important role in systemic aging.

Supplementary Material

Supplementary data are available at *The Journals of Gerontology, Series A: Biological Sciences and Medical Sciences* online.

Funding

This work was supported by the National Key R&D Program of China (grant number 2020YFC2008000); the National Natural Science Foundation of China Youth Science Fund Project (grant number 82101635); and the National Natural Science Foundation of China (grant number 81873811).

Conflict of Interest

None.

Data Availability

The data that support the findings of this study are included in the article. Raw data used to generate the figures are available from the corresponding author upon request.

Author Contributions

H.L., L.Z., J.Y., and C.Z. conceived the study and designed the experiments. H.L., Z.Y., and W.L. performed the experiments. H.L., H.N., Y.G., N.Y., and T.J. analyzed the data. Y.L. and Y.H. prepared the figures. H.L. and Z.Y. wrote the first version of the manuscript. J.Y. made logical and content revisions to the manuscript. All authors approved the final version of the manuscript.

References

- Li YJ, Jin X, Li D, et al. New insights into vascular aging: emerging role of mitochondria function. *Biomed Pharmacother.* 2022;156:113954. <https://doi.org/10.1016/j.biopha.2022.113954>
- Hooglugt A, Klatt O, Huveners S. Vascular stiffening and endothelial dysfunction in atherosclerosis. *Curr Opin Lipidol.* 2022;33:353–363. <https://doi.org/10.1097/MOL.0000000000000852>
- Badaras I, Laučytė-Cibulskienė A. Vascular aging and COVID-19. *Angiology.* 2022;74:308–316. <https://doi.org/10.1177/00033197221121007>
- Guo Y, Xu A, Wang Y. SIRT1 in endothelial cells as a novel target for the prevention of early vascular aging. *J Cardiovasc Pharmacol.* 2016;67:465–473. <https://doi.org/10.1097/FJC.0000000000000344>
- Donato AJ, Morgan RG, Walker AE, Lesniewski LA. Cellular and molecular biology of aging endothelial cells. *J Mol Cell Cardiol.* 2015;89:122–135. <https://doi.org/10.1016/j.yjmcc.2015.01.021>
- Hwang HJ, Kim N, Herman AB, Gorospe M, Lee JS. Factors and pathways modulating endothelial cell senescence in vascular aging. *Int J Mol Sci.* 2022;23:10135. <https://doi.org/10.3390/ijms231710135>
- Pantsulaia I, Ciszewski WM, Niewiarowska J. Senescent endothelial cells: potential modulators of immunosenescence and ageing. *Ageing Res Rev.* 2016;29:13–25. <https://doi.org/10.1016/j.arr.2016.05.011>
- Jia G, Aroor AR, Jia C, Sowers JR. Endothelial cell senescence in aging-related vascular dysfunction. *Biochim Biophys Acta Mol Basis Dis.* 2019;1865:1802–1809. <https://doi.org/10.1016/j.bbdis.2018.08.008>
- Gao Q, Chen K, Gao L, Zheng Y, Yang YG. Thrombospondin-1 signaling through CD47 inhibits cell cycle progression and induces senescence in endothelial cells. *Cell Death Dis.* 2016;7:e2368. <https://doi.org/10.1038/cddis.2016.155>
- Xu C, Wang L, Fozzouni P, et al. SIRT1 is downregulated by autophagy in senescence and ageing. *Nat Cell Biol.* 2020;22:1170–1179. <https://doi.org/10.1038/s41556-020-00579-5>
- Nikolajevic J, Ariaee N, Liew A, Abbasnia S, Fazeli B, Sabovic M. The role of microRNAs in endothelial cell senescence. *Cells.* 2022;11:1185. <https://doi.org/10.3390/cells11071185>
- Zerenturk EJ, Sharpe LJ, Ikonen E, Brown AJ. Desmosterol and DHCR24: unexpected new directions for a terminal step in cholesterol synthesis. *Prog Lipid Res.* 2013;52:666–680. <https://doi.org/10.1016/j.plipres.2013.09.002>
- Waterham HR, Koster J, Romeijn GJ, et al. Mutations in the β -hydroxysterol Δ 24-reductase gene cause desmosterolosis, an autosomal recessive disorder of cholesterol biosynthesis. *Am J Hum Genet.* 2001;69:685–694. <https://doi.org/10.1086/323473>
- Iivonen S, Hiltunen M, Alafuzoff I, et al. Seladin-1 transcription is linked to neuronal degeneration in Alzheimer's disease. *Neuroscience.* 2002;113:301–310. [https://doi.org/10.1016/s0306-4522\(02\)00180-x](https://doi.org/10.1016/s0306-4522(02)00180-x)
- Bai X, Mai M, Yao K, et al. The role of DHCR24 in the pathogenesis of AD: re-cognition of the relationship between cholesterol and AD pathogenesis. *Acta Neuropathol Commun.* 2022;10:35. <https://doi.org/10.1186/s40478-022-01338-3>
- Gokani S, Bhatt LK. Caveolin-1: a promising therapeutic target for diverse diseases. *Curr Mol Pharmacol.* 2022;15:701–715. <https://doi.org/10.2174/1874467214666211130155902>
- Enyong EN, Gurley JM, De Ieso ML, Stamer WD, Elliott MH. Caveolar and non-caveolar caveolin-1 in ocular homeostasis and disease. *Prog Retin Eye Res.* 2022;91:101094. <https://doi.org/10.1016/j.preteyeres.2022.101094>
- Jiang X, Li Y, Fu D, et al. Caveolin-1 ameliorates acetaminophen-aggravated inflammatory damage and lipid deposition in non-alcoholic fatty liver disease via the ROS/TXNIP/NLRP3 pathway. *Int Immunopharmacol.* 2023;114:109558. <https://doi.org/10.1016/j.intimp.2022.109558>
- Lu X, Kambe F, Cao X, et al. DHCR24-knockout embryonic fibroblasts are susceptible to serum withdrawal-induced apoptosis because of dysfunction of caveolae and insulin-Akt-Bad signaling. *Endocrinology.* 2006;147:3123–3132. <https://doi.org/10.1210/en.2005-1426>
- Wary KK, Mariotti A, Zurzolo C, Giancotti FG. A requirement for caveolin-1 and associated kinase Fyn in integrin signaling and anchorage-dependent cell growth. *Cell.* 1998;94:625–634. [https://doi.org/10.1016/s0092-8674\(00\)81604-9](https://doi.org/10.1016/s0092-8674(00)81604-9)
- Xu L, Wang L, Wen Z, et al. Caveolin-1 is a checkpoint regulator in hypoxia-induced astrocyte apoptosis via Ras/Raf/ERK pathway. *Am J Physiol Cell Physiol.* 2016;310:C903–C910. <https://doi.org/10.1152/ajpcell.00309.2015>
- Park JH, Ryu JM, Han HJ. Involvement of caveolin-1 in fibronectin-induced mouse embryonic stem cell proliferation: role of FAK, RhoA, PI3K/Akt, and ERK 1/2 pathways. *J Cell Physiol.* 2011;226:267–275. <https://doi.org/10.1002/jcp.22338>
- Codenotti S, Marampon F, Triggiani L, et al. Caveolin-1 promotes radioresistance in rhabdomyosarcoma through increased oxidative stress protection and DNA repair. *Cancer Lett.* 2021;505:1–12. <https://doi.org/10.1016/j.canlet.2021.02.005>
- Jiang Y, Krantz S, Qin X, et al. Caveolin-1 controls mitochondrial damage and ROS production by regulating fission—fusion dynamics and mitophagy. *Redox Biol.* 2022;52:102304. <https://doi.org/10.1016/j.redox.2022.102304>
- Yan J, Wang J, Huang H, et al. Fibroblast growth factor 21 delayed endothelial replicative senescence and protected cells from H₂O₂-induced premature senescence through SIRT1. *Am J Transl Res.* 2017;9:4492–4501.
- Sobczak M, Dargatz J, Chrzanowska-Wodnicka M. Isolation and culture of pulmonary endothelial cells from neonatal mice. *J Vis Exp.* 2010;46:2316. <https://doi.org/10.3791/2316>
- Ke Y, Li D, Zhao M, et al. Gut flora-dependent metabolite trimethylamine-N-oxide accelerates endothelial cell senescence and vascular aging through oxidative stress. *Free Radic Biol Med.* 2018;116:88–100. <https://doi.org/10.1016/j.freeradbiomed.2018.01.007>
- Hernandez-Segura A, Nehme J, Demaria M. Hallmarks of cellular senescence. *Trends Cell Biol.* 2018;28:436–453. <https://doi.org/10.1016/j.tcb.2018.02.001>
- Ogrodnik M. Cellular aging beyond cellular senescence: markers of senescence prior to cell cycle arrest in vitro and in vivo. *Ageing Cell.* 2021;20:e13338. <https://doi.org/10.1111/acel.13338>
- Si Z, Sun L, Wang X. Evidence and perspectives of cell senescence in neurodegenerative diseases. *Biomed Pharmacother.* 2021;137:111327. <https://doi.org/10.1016/j.biopha.2021.111327>
- Jin SW, Pham HT, Choi JH, et al. Impressic acid, a lupane-type triterpenoid from *acanthopanax koreanum*, attenuates TNF- α -induced endothelial dysfunction via activation of eNOS/NO pathway. *Int J Mol Sci.* 2019;20:5772. <https://doi.org/10.3390/ijms20225772>
- Dong ZC, Wu MM, Zhang YL, et al. The vascular endothelial growth factor trap aflibercept induces vascular dysfunction and

- hypertension via attenuation of eNOS/NO signaling in mice. *Acta Pharmacol Sin.* 2021;42:1437–1448. <https://doi.org/10.1038/s41401-020-00569-1>
33. Huang Y, Zhang W, Guo X, Zhang Y, Wu J, Zu H. Cellular cholesterol loss by DHCR24 knockdown leads to Abeta production by changing APP intracellular localization. *J Lipid Res.* 2023;64:100367. <https://doi.org/10.1016/j.jlr.2023.100367>
 34. Bai X, Wu J, Zhang M, et al. DHCR24 knock-down induced tau hyperphosphorylation at Thr181, Ser199, Thr231, Ser262, Ser396 epitopes and inhibition of autophagy by overactivation of GSK3 β /mTOR signaling. *Front Aging Neurosci.* 2021;13:513605. <https://doi.org/10.3389/fnagi.2021.513605>
 35. Liu RM. Aging, cellular senescence, and Alzheimer's disease. *Int J Mol Sci.* 2022;23:1989. <https://doi.org/10.3390/ijms23041989>
 36. Sharpe LJ, Wong J, Garner B, Halliday GM, Brown AJ. Is seladin-1 really a selective Alzheimer's disease indicator? *J Alzheimers Dis.* 2012;30:35–39. <https://doi.org/10.3233/JAD-2012-111955>
 37. Gortazar AR, Martin-Millan M, Bravo B, Plotkin LI, Bellido T. Crosstalk between caveolin-1/extracellular signal-regulated kinase (ERK) and beta-catenin survival pathways in osteocyte mechanotransduction. *J Biol Chem.* 2013;288:8168–8175. <https://doi.org/10.1074/jbc.M112.437921>
 38. Liu W, Jiang P, Qiu L. Blocking of caveolin-1 attenuates morphine-induced inflammation, hyperalgesia, and analgesic tolerance via inhibiting NLRP3 inflammasome and ERK/c-JUN pathway. *J Mol Neurosci.* 2022;72:1047–1057. <https://doi.org/10.1007/s12031-022-01989-w>
 39. Zhang C, Wu Q, Huang H, et al. Caveolin-1 promotes Rfng expression via Erk-Jnk-p38 signaling pathway in mouse hepatocarcinoma cells. *J Physiol Biochem.* 2019;75:549–559. <https://doi.org/10.1007/s13105-019-00703-6>
 40. Boothe T, Lim GE, Cen H, et al. Inter-domain tagging implicates caveolin-1 in insulin receptor trafficking and Erk signaling bias in pancreatic beta-cells. *Mol Metab.* 2016;5:366–378. <https://doi.org/10.1016/j.molmet.2016.01.009>
 41. Shim H, Shim E, Lee H, et al. CAGE, a novel cancer/testis antigen gene, promotes cell motility by activation ERK and p38 MAPK and downregulating ROS. *Mol Cells.* 2006;21:367–375.
 42. Le AN, Park SS, Le MX, et al. DRG2 depletion promotes endothelial cell senescence and vascular endothelial dysfunction. *Int J Mol Sci.* 2022;23:2877. <https://doi.org/10.3390/ijms23052877>
 43. Xiao HB, Sui GG, Lu XY. Icaritin improves eNOS/NO pathway to prohibit the atherogenesis of apolipoprotein E-null mice. *Can J Physiol Pharmacol.* 2017;95:625–633. <https://doi.org/10.1139/cjpp-2016-0367>
 44. Genaro-Mattos TC, Anderson A, Allen LB, Korade Z, Mirnic K. Cholesterol biosynthesis and uptake in developing neurons. *ACS Chem Neurosci.* 2019;10:3671–3681. <https://doi.org/10.1021/acscchemneuro.9b00248>
 45. Simonen P, Li S, Chua NK, et al. Amiodarone disrupts cholesterol biosynthesis pathway and causes accumulation of circulating desmosterol by inhibiting 24-dehydrocholesterol reductase. *J Intern Med.* 2020;288:560–569. <https://doi.org/10.1111/joim.13095>
 46. Gilk SD, Cockrell DC, Luterbach C, et al. Bacterial colonization of host cells in the absence of cholesterol. *PLoS Pathog.* 2013;9:e1003107. <https://doi.org/10.1371/journal.ppat.1003107>
 47. Heverin M, Meaney S, Brafman A, et al. Studies on the cholesterol-free mouse: strong activation of LXR-regulated hepatic genes when replacing cholesterol with desmosterol. *Arterioscler Thromb Vasc Biol.* 2007;27:2191–2197. <https://doi.org/10.1161/ATVBAHA.107.149823>
 48. Sun S, Qin W, Tang X, et al. Vascular endothelium-targeted Sirt7 gene therapy rejuvenates blood vessels and extends life span in a Hutchinson-Gilford progeria model. *Sci Adv.* 2020;6:eaay5556. <https://doi.org/10.1126/sciadv.aay5556>